

Engineering Notes

ENGINEERING NOTES are short manuscripts describing new developments or important results of a preliminary nature. These Notes cannot exceed 6 manuscript pages and 3 figures; a page of text may be substituted for a figure and vice versa. After informal review by the editors, they may be published within a few months of the date of receipt. Style requirements are the same as for regular contributions (see inside back cover).

Combined Effects of Nose Bluntness and Surface Perturbations on Asymmetric Flow Past Slender Bodies

C. A. Moskovitz*

Virginia Polytechnic Institute and State University,
Blacksburg, Virginia

R. M. Hall†

NASA Langley Research Center, Hampton, Virginia
and

F. R. DeJarnette‡

North Carolina State University,
Raleigh, North Carolina

Introduction

IN recent years, increased emphasis has been placed on understanding the complicated, asymmetric vortex flowfields that occur over aircraft and missile noses at large angles of attack. Previous researchers¹ have disclosed much of the physics of these flows and have developed some new theories of asymmetric flow behavior. The data to be discussed here were intended to verify some of the existing but unproven theories summarized in Ref. 1, and, in addition, to provide new information to further refine those theories.

This experimental investigation studied the effects of variations in model tip sharpness with and without the discrete surface perturbations of cylindrical beads attached to the model surface. Also investigated were variations in tip roughness, which are not discussed here due to space limitations. The complete data (including roughness data and flow visualization) can be found in Ref. 2.

Results and Conclusions

A cone/cylinder model with a 10-deg semiapex angle and a 3.0-caliber tangent-ogive model were tested at laminar flow conditions at angles of attack from 30 to 60 deg. Data were taken with each model from three circumferential rows of pressure taps at a Reynolds number of 8.40×10^4 based on the cylinder diameter of 3.5 in. The beads were tested with a variety of tips (Fig. 1) that were attached at varying axial and azi-

muthal (ϕ_b) positions and were measured from the apex and windward ray, respectively. The impact of the beads was judged by the extent to which the flowfield was affected.

Samples of data from tests of the cone and ogive models with various tips are presented. The pressure distributions from each ring of pressure taps were integrated to give values of the sectional side-force coefficient C_y at each of the ring locations. These are shown as rows 1, 2, and 3 in Figs. 2-4 with row 1 being closest to the apex.

Figure 2 shows a comparison of the distributions of C_y with model roll position (ϕ_m) for cone tips 8 and 9, which were nominally machined to the same geometry. Note that these distributions are highly dissimilar, except for the magnitude of the maximum C_y . These results are representative of all tips tested on both models and were highly repeatable, showing the significance of minute surface irregularities, due to, in this case, the imperfect machining processes.

Similar results are seen in Fig. 3, which compares the data of sharp ogive tips 1 and 3 and blunted tips 4 and 5. The decreased maximum C_y due to the blunter tips can be seen in Fig. 3, as has been shown previously by many researchers. The importance lies in the comparison of these data with that of Fig. 4. Here, for each tip, the ogive model was placed at a roll position that resulted in a nearly symmetric flowfield. The plastic

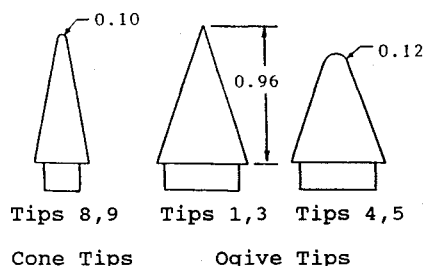


Fig. 1 Dimensions of cone and ogive tips (in.).

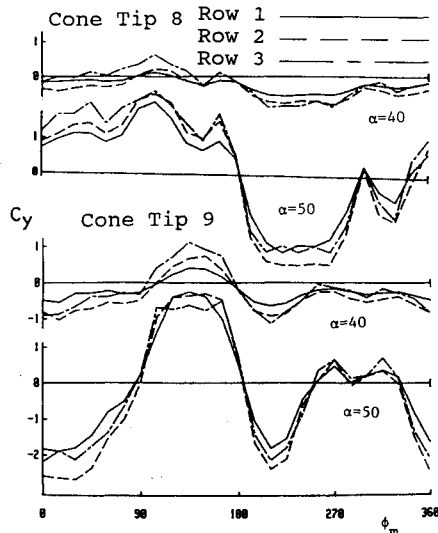


Fig. 2 Cone tips 8 and 9: Variation of sectional side-force coefficient with model roll position.

Received May 25, 1989; presented as Paper 89-2236 at the AIAA 7th Applied Aerodynamics Conference, Seattle, WA, July 31-Aug. 2, 1989; revision received June 12, 1990; accepted for publication June 12, 1990. Copyright © 1990 by the American Institute of Aeronautics and Astronautics, Inc. No copyright is asserted in the United States under Title 17, U.S. Code. The U.S. Government has a royalty-free license to exercise all rights under the copyright claimed herein for Governmental purposes. All other rights are reserved by the copyright owner.

*Research Associate, Aerospace and Ocean Engineering. Member AIAA.

†Senior Research Engineer. Associate Fellow AIAA.

‡Professor, Mechanical and Aerospace Engineering. Associate Fellow AIAA.

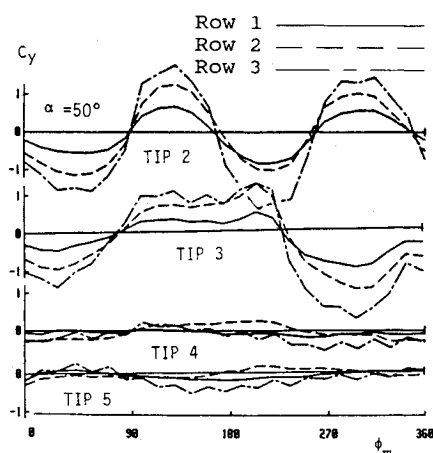


Fig. 3 Ogive tips 1, 3, 4, and 5: Variation of sectional side-force coefficient with model roll position.

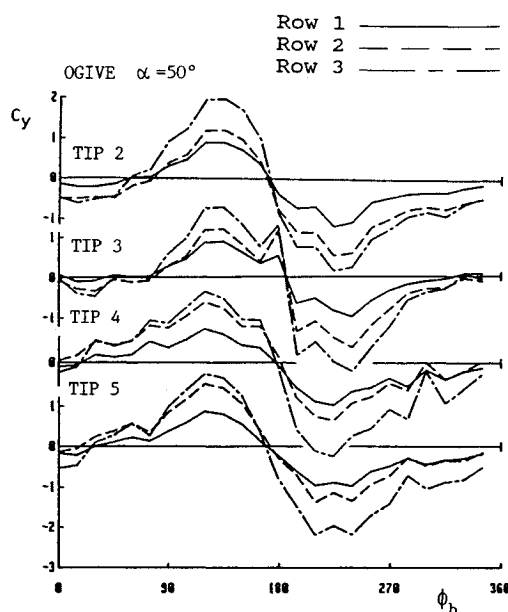


Fig. 4 Effect of tip shape on variation of sectional side-force coefficient with circumferential bead position.

bead was placed at varying azimuthal locations in 15-deg increments, all at a fixed axial position of 1.0 in., which corresponded to the tip/body junction. The bead was $\frac{1}{8}$ in. high with a diameter of $\frac{1}{8}$ in. Note that both the shape of the side-force distributions and the maximum values were nearly identical for all tips, including the blunter ones. The large side forces observed when the bead was nearly 45 deg from the windward ray indicates that blunt tips may produce as much flowfield asymmetry as sharper tips, if equivalent model asymmetry is present.

Previous research by the authors³ has shown that the effect of a singular roughness element is proportional to the element's size relative to the dimensions of the body where the roughness occurs. Therefore, reductions in side force with bluntness are largely the result of three factors. First, surface imperfections on a blunt tip are smaller relative to the tip diameter at which they occur than the same disturbances would be on the apex of a sharper tip. Second, machining processes are less likely to produce irregularities on a sturdy blunt tip than on a relatively flimsy sharp one. Third, blunter tips are more difficult to damage and, therefore, more likely to keep their shape. Microscopic photographs of some of the tips tested, showing machining imperfections, can be seen in Ref. 2.

References

- ¹Hunt, B. L., "Asymmetric Vortex Forces and Wakes on Slender Bodies," AIAA Paper 82-1336, Aug. 1982.
- ²Moskovitz, C. A., Hall, R. M., and DeJarnette, F. R., "Effects of Nose Bluntness, Roughness and Surface Perturbations on the Asymmetric Flow Past Slender Bodies at Large Angles of Attack," AIAA Paper 89-2236, Aug. 1989.
- ³Moskovitz, C. A., Hall, R. M., and DeJarnette, F. R., "Effects of Surface Perturbations on the Asymmetric Vortex Flow Over a Slender Body," AIAA Paper 88-0483, Jan. 1988.

Accurate Method for Calculating Initial Development of Vortex Sheets

Rajendra K. Bera*

National Aeronautical Laboratory,
Bangalore, India

Introduction

IN this Note, the dynamics of a planar, infinitesimally thin, finite-span vortex sheet placed at time $t = 0$ in an otherwise unbounded stationary fluid is studied for small times, $t > 0$. The solution is expressed as a power series in time whose coefficients are calculated accurately by a proper numerical evaluation of the accompanying Cauchy integrals. The method does not discretize the vortex sheet and is the numerical counterpart of the semianalytical method of Ref. 1.

The more difficult problem—when the vortex sheet is curved at $t = 0$ —has been addressed in Ref. 2 using a time-marching scheme. This method is computationally expensive because very small time steps are required to maintain accuracy. In comparison, for the initially plane vortex sheet, the method presented herein is at least three orders of magnitude faster. It also serves the long-felt need to determine rapidly the initial development of an aircraft wing wake to engineering accuracy, for which the two-dimensional vortex sheet is considered a reasonable model.^{3,4}

Problem Statement

Consider a two-dimensional free vortex sheet whose vorticity vector is perpendicular to the x, y plane and whose Trefftz plane cross section at some instant $t = 0$ spans the line $-1 \leq x \leq 1$, $y = 0$. Let the sheet vorticity distribution be $G(x)$. At any instant $t > 0$, let $[X(x, t), Y(x, t)]$ be the coordinates of the fluid element originally located at $(x, 0)$ at $t = 0$. The convective motion of the vortex sheet is then governed by

$$u(x, t) = \frac{dX}{dt} = -\left(\frac{1}{2}\pi\right) \int_{-1}^1 S^{-1}(x, \xi, t) \times G(\xi) [Y(x, t) - Y(\xi, t)] d\xi \quad (1a)$$

$$v(x, t) = \frac{dY}{dt} = \left(\frac{1}{2}\pi\right) \int_{-1}^1 S^{-1}(x, \xi, t) \times G(\xi) [X(x, t) - X(\xi, t)] d\xi \quad (1b)$$

where use has been made of the fact that, in an incompressible, inviscid, two-dimensional fluid flow, vorticity is a passively convected scalar. Furthermore, $u(x, t)$ and $v(x, t)$ are the x and y components, respectively, of the sheet convection veloc-

Received Oct. 27, 1989; revision received April 16, 1990; accepted for publication April 30, 1990. Copyright © 1990 by Rajendra K. Bera. Published by the American Institute of Aeronautics and Astronautics, Inc., with permission.

*Scientist, Computational and Theoretical Fluid Dynamics Division.